INTERNATIONAL TRANSACTIONS
IN OPERATIONAL RESEARCH

INTERNATIONAL
TRANSACTIONS
IN OPERATIONAL
RESEARCH

WILEY

An automated treatment planning strategy for highly noncoplanar radiotherapy arc trajectories

P. Carrasqueira[a,*] iD, H. Rocha[a,b] iD, J. M. Dias[a,b], T. Ventura[a,c], B. C. Ferreira[a,d]
and M. C. Lopes[a,c] iD

[a] University of Coimbra, INESCC, Rua Silvio Lima, Coimbra 3030-290, Portugal
[b] University of Coimbra, FEUC, CeBER, Av. Dias da Silva 165, Coimbra 3004-512, Portugal
[c] IPOC-FG, EPE, Av. Bissaya Barreto 98, Coimbra 3000-075, Portugal
[d] ESS-PP, Rua Valente Perfeito 322, Vila Nova de Gaia 4400-330, Portugal
E-mail: pedro.carrasqueira@deec.uc.pt [Carrasqueira]; hrocha@fe.uc.pt [Rocha]; joana@fe.uc.pt [Dias];
tiagoventura@ipocoimbra.min-saude.pt [Ventura]; bcf@ess.ipp.pt [Ferreira]; mclopes@ipocoimbra.min-saude.pt
[Lopes]

Abstract

Radiation therapy is a technology-driven cancer treatment modality that has experienced significant advances over the last decades, due to multidisciplinary contributions that include engineering and computing. Recent technological developments allow the use of noncoplanar volumetric modulated arc therapy (VMAT), one of the most recent photon treatment techniques, in clinical practice. In this work, an automated noncoplanar arc trajectory optimization framework designed in two modular phases is presented. First, a noncoplanar beam angle optimization algorithm is used to obtain a set of noncoplanar irradiation directions. Then, anchored in these directions, an optimization strategy is proposed to compute an optimal arc trajectory. The computational experiments considered a pool of twelve difficult head-and-neck tumor cases. It was possible to observe that, for some of these cases, the optimized noncoplanar arc trajectories led to significant treatment planning quality improvements, when compared with coplanar VMAT treatment plans. Although these experiments were done in a research environment treatment planning software (matRad), the conclusions can be of interest for a clinical setting: automated procedures can simplify the current treatment workflow, produce high-quality treatment plans, making better use of human resources and allowing for unbiased comparisons between different treatment techniques.

Keywords: radiation therapy; noncoplanar arc therapy; optimization; automation

1. Introduction

Cancer continues to be an increasing health problem with an expected increase in 63.1% of cancer cases by 2040 compared to 2018 (WHO). In high-income countries, photon radiation therapy (RT)

[Correction added on August 11, 2021, after first online publication: The copyright line was changed.]

*Corresponding author.

is used in more than half of all cancer cases (Atun et al., 2015). The goal of RT is to eliminate all cancerous cells by irradiating the tumor volume(s) Planning target volume (PTVs) with a prescribed radiation dose while trying to spare the surrounding organs at risk (OARs) as much as possible. In external RT, radiation is generated by a linear accelerator mounted on a gantry able to rotate around the patient who lays immobilized in a treatment couch that can also rotate around a vertical axis that intersects the gantry rotation horizontal axis at a point called the isocenter. The rotation of the couch and the gantry allows the irradiation of the tumor from almost any direction. The possibility of selecting appropriate noncoplanar irradiation directions—noncoplanar beam angle optimization (BAO) problem—can enhance treatment plan quality, particularly for complex tumor sites as head-and-neck cancer cases (Bangert et al., 2013).

RT has seen considerable changes in the last decades, offering an increased range of treatment techniques to cancer patients. The most advanced RT systems use a multileaf collimator (MLC) to modulate the radiation beam into a discrete set of small beamlets with different intensities. The beamlet intensities can be optimized—fluence map optimization (FMO) problem—leading to nonuniform radiation fields that can be sequenced and delivered while the gantry is halted at the given beam irradiation directions, static intensity-modulated radiation therapy (IMRT), or can be delivered while the gantry rotates around the patient with the treatment beam always on, rotational/arc IMRT. VMAT is one of the most efficient IMRT arc techniques, particularly with respect to dose delivery time (Otto, 2008). Typically, VMAT uses coplanar beam trajectories, performed for a fixed couch angle (usually 0°).

Recent technological advances give additional degrees of freedom to treatment planning. Moving simultaneously the gantry and the couch, provided collisions are avoided, has become a reality for the most recent line of linear accelerators. Highly noncoplanar arc trajectories can now be obtained as couch rotation is allowed while the gantry rotates around the patient. Recently, the use of highly noncoplanar trajectories was proposed to combine the benefits of VMAT, such as short treatment times (Otto, 2008), with the benefits of noncoplanar IMRT treatment plans, such as improved organ sparing (Bangert et al., 2013).

Designing a complete end-to-end noncoplanar VMAT treatment plan requires different optimization problems to be addressed, related to beam angle selection, FMO, and trajectory optimization, in order to increase treatment plan quality. To obtain a deliverable treatment plan, it is also needed to adapt the treatment plan to specific constraints of the machine. In Yang et al. (2011), a new method is presented to deal with dynamic movement of gantry and couch, as the dose is being delivered to the patient. A geometric-based score is proposed to measure the OARs overlapping the tumor indicating promising trajectories. Hierarchical clustering is then used to construct multiple subarcs with continuous gantry and couch rotation. MacDonald and Thomas (2015) embedded beams-eye-view dose metrics, that is, metrics related to the percentage of PTV and OARs seen from each beam direction, in their arc trajectory optimization. Smyth et al. (2016) also considered a geometric-based heuristic to select noncoplanar beams, relying on a cost function that evaluates the OARs superposition with the PTV, for each beam. Considering the score determined for each beam, the shortest path Dijkstra algorithm is used to design the final noncoplanar trajectory. This technique makes some improvements on the approach presented in Smyth et al. (2013), namely assigning different weights to each OAR according to its relative importance. Papp et al. (2015) presented an approach to obtain noncoplanar VMAT treatment plans that start by performing beam angle selection resorting to two FMO heuristics. The beam trajectory is obtained by

optimizing distances considered as the sum of the time needed to change from one beam to the next, for all the trajectories, resorting to the shortest path algorithm. In Wild et al. (2015) the non-coplanar VMAT trajectories were constructed using genetic algorithms to solve the shortest path problem based on the anchor points given by the beams of noncoplanar IMRT plans. Langhans et al. (2018) designed a strategy to perform noncoplanar BAO and then used a geometrical-based metric to find an optimized arc trajectory.

In this paper, a completely automated approach to obtain a noncoplanar VMAT treatment plan is described. Initially, a noncoplanar beam angle optimized solution is determined lying on a strategy early developed (Rocha et al., 2016, 2019a). Anchored on the noncoplanar beam directions calculated, an automated fluence-based optimization framework is proposed for obtaining an optimal noncoplanar arc trajectory plan. An experimental direct aperture optimization (DAO) implementation provided by matRad (Wieser et al., 2017) is used for fluence optimization that guides both BAO and trajectory optimization, aiming at minimizing the possible discrepancies to fully deliverable VMAT plans. An initial proof of concept for this methodological approach has been presented in Rocha et al. (2019b). In this previous work, only one nasopharyngeal tumor case was considered, and the arc trajectory was manually calculated. Moreover, the conventional beamlet-based fluence optimization was used, which is not the best approach when considering VMAT treatments (Unkelbach et al., 2015). The results obtained in the preliminary study motivated us to pursuit a completely automated procedure for arc trajectory optimization. In the current work, an automated methodology integrating BAO, FMO resorting to DAO, and arc trajectory optimization are presented. The approach herein presented is assessed in a group of 12 head-and-neck cancer patients already treated at the Portuguese Institute of Oncology of Coimbra (IPOC). The obtained results show that it is possible to reach high-quality treatment plans for difficult cases with the least human intervention possible. Although all the experiments were made in a research environment treatment planning software (matRad), the methodological choices made bridge the gap between the research environment and the clinical setting. This paper is organized as follows. In Section 2, the head-and-neck cancer cases used to assess the proposed approach are presented. The trajectory optimization framework is described in Section 3. In Section 4, the computational results are presented. The last section is devoted to the conclusions.

2. Head-and-neck cancer cases

Twelve head-and-neck complex tumor cases already treated at IPOC were considered to assess the proposed automated approach. Two different dose prescription levels were considered for each patient. A higher radiation dose of 70.0 Gy was prescribed to the tumor (PTV_{70}), while a lower radiation dose of 59.4 Gy was prescribed to the lymph nodes ($PTV_{59.4}$).

Treatment planning of head-and-neck cancer cases is difficult due to the large number of OARs surrounding both tumor and lymph nodes. Parotid glands, oral cavity, spinal cord, and brainstem compose the list of OARs considered. The larger salivary glands, left and right parotids, and the oral cavity, which contains the remaining salivary glands, are parallel organs, that is, organs whose functionality is not impaired if only a small part is damaged. Thus, mean-dose constraints are considered for these organs. Spinal cord and brainstem are serial organs, that is, organs that may see their functionality impaired even if only a small part is damaged. Thus, maximum-dose constraints

Table 1
Prescribed doses for the PTVs and tolerance doses for the OARs considered

Structure	Prescribed dose	Tolerance Dose	
		Mean	Max
PTV_{70}	70.0 Gy	–	–
$PTV_{59.4}$	59.4 Gy	–	–
Left parotid	–	26 Gy	–
Right parotid	–	26 Gy	–
Oral cavity	–	45 Gy	–
Spinal cord	–	–	45 Gy
Brainstem	–	–	54 Gy
Body	–	–	75 Gy

have to be considered. A structure containing the remaining normal tissues, Body, is also considered to prevent dose accumulation elsewhere. Table 1 depicts the prescribed doses for the PTVs and the tolerance doses for the OARs considered.

3. Noncoplanar arc trajectory optimization framework

The proposed arc trajectory optimization framework is an automated modular process that evolves in two steps. In the first step, a set of optimal noncoplanar beam irradiation directions is obtained, resorting to a previously developed BAO algorithm (Rocha et al., 2016, 2019a). In the second step, anchored in the previously computed beam directions, additional beam directions are iteratively calculated in order to define the noncoplanar arc trajectory. The optimization procedures of both steps are guided by the optimal value of the fluence optimization problem. DAO is used in this work for fluence optimization rather than the conventional beamlet-based fluence optimization commonly used.

3.1. Fluence map optimization—direct aperture optimization

In arc therapy, the gantry rotates around the patient with the beam always on while the gantry speed, dose rate, and aperture shaped by the MLC are modulated. Figure 1 illustrates an MLC with different aperture shapes and the corresponding radiation maps whose superimposition originates a nonlinear fluence map. Conventional fluence optimization calculates the optimal intensities of each beamlet that produces the nonlinear intensity map. In order to be deliverable, another optimization step is required to calculate the sequence of apertures (sequencing) that approximately reproduce the optimal nonlinear fluence maps. DAO calculates aperture shapes instead of beamlet intensities producing a deliverable plan. The use of DAO during treatment planning can thus decrease possible discrepancies to fully deliverable VMAT plans.

The head-and-neck clinical cases considered in this work were assessed in matRad (Wieser et al., 2017). matRad is an open source multimodality radiation treatment planning system, written in
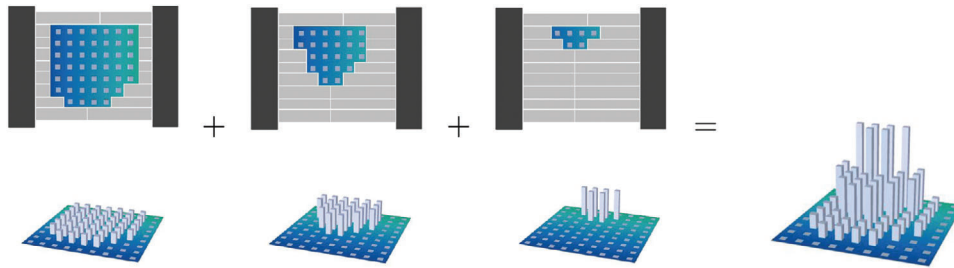
Fig. 1. Illustration of an MLC with different apertures and corresponding radiation maps whose superimposition originates a nonlinear fluence map.

Matlab, developed at the German Cancer Research Center. Core functionalities comprising matRad include importing Digital Imaging and Communications in Medicine data, dose calculation, and optimization as well as a graphical user interface for visualization. It comprehends twofold usage, writing customized Matlab scripts or using matRad GUI, which provides a straightforward process to obtain a treatment plan through a completely automated procedure. Fluence optimization in matRad may be customized selecting, from a set of options available, objectives, constraints, or weights assigned to each structure. Thus, matRad provides the necessary flexibility to design a custom optimization procedure in an automated fashion. Furthermore, matRad provides an experimental DAO implementation, which was the main motivation to use this software in this work. matRad uses a gradient-based DAO algorithm (Cassioli and Unkelbach, 2013) that depends on a good starting solution. Therefore, a conventional fluence optimization including sequencing (Xia and Verhey, 1998) is first performed and the resulting segments are then refined based on gradient information (Wieser et al., 2017).

In this work, a convex voxel-based nonlinear model (Yang and Xing, 2004; Aleman et al., 2008) is used for fluence optimization by selecting the appropriate options in matRad. The individual objective functions used to assess each structure are available by default in matRad and were parameterized by us to build the selected nonlinear model. In this model, the objective function accounts for the overall penalization considering the weighted sum of square deviation of the dose deposited in each voxel relatively to the dose prescribed for that voxel. This evaluation is performed for each structure s of the S structures considered. The mathematical formulation results in a quadratic programming problem. For each structure s, the objective function is formulated as

$$f_s(w) = \underline{\lambda}_s \left(T_s - \sum_{j=1}^{N_b} D_{ij} w_j \right)_+^2 + \overline{\lambda}_s \left(\sum_{j=1}^{N_b} D_{ij} w_j - T_s \right)_+^2, \tag{1}$$

where D_{ij} is the unitary dose delivered to voxel i by beamlet j, w_j is the weight (intensity) of beamlet j, T_s is the prescribed/tolerance dose of structure s, N_b is the number of beamlets, $\underline{\lambda}_s$ and $\overline{\lambda}_s$ are the lower and upper penalties for structure s, and $(\cdot)_+ = \max\{0, \cdot\}$. The unitary dose was computed using matRad's pencil beam algorithm. The underdosage has not been penalized for OARs, which means setting $\underline{\lambda}_s$ null for those structures. In matRad, an importance rank k_s is assigned to each structure s. If a voxel belongs to more than one structure, for optimization purposes, it is assigned

to the most important structure. Higher importance ranks, k_s, were assigned to PTVs ($k_s = 1$), followed by the OARs ($k_s = 2$). The lowest importance rank was assigned to remaining normal tissues (k_s was set to 3 for Body). The FMO model is obtained by the weighted sum of the objective functions defined for the structures.

In matRad, the fluence optimization problem is solved resorting to the interior point optimizer solver IPOPT (Wachter and Biegler, 2006), which is a reliable free software package developed by the COIN-OR initiative fitted to solve large-scale nonlinear constrained optimization problems. IPOPT is made available by a MEX file, which considers the objective functions and constraints defined within the matRad environment.

3.2. Noncoplanar beam angle selection

In clinical practice, equispaced coplanar irradiation directions are still commonly used, that is, beam irradiation directions evenly distributed on the plane of rotation of the linear accelerator's gantry. The main reason for the clinical use of equispaced beam angle ensembles is inherent to the challenge of solving the BAO problem, a nonconvex problem with many local minima on a large search space (Craft, 2007). The vast majority of the approaches proposed to address the BAO problem consider a discrete subset of all continuous beam angle directions solving the resulting combinatorial optimization problem (Pugachev et al., 2001; Aleman et al., 2008; Lim and Cao, 2012; Bertsimas et al., 2013; Dias et al., 2014, 2015; Cabrera et al., 2018; Freitas et al., 2020), either relying on geometric measures or in dosimetric values. However, the optimal solution of the combinatorial BAO problem cannot be calculated in a polynomial run time—NP-hard problem (Bangert et al., 2012). We proposed an alternative BAO formulation. Instead of considering a discrete subset of beam directions, all continuous beam angle directions are considered leading to a continuous global optimization problem (Rocha et al., 2016, 2019a). The continuous formulation and resolution of the noncoplanar BAO problem is briefly described next.

Considering the goal of obtaining a beam ensemble with n beams and assuming that θ stands for the gantry angle and ϕ for the couch angle, the noncoplanar BAO problem can be simply formulated as

$$\min \quad f((\theta_1, \phi_1), (\theta_2, \phi_2), \dots, (\theta_n, \phi_n))$$
$$s.t. \quad (\theta_1, \phi_1), (\theta_2, \phi_2), \dots, (\theta_n, \phi_n) \in A,$$

where $A = \{(\theta, \phi) : \theta \in [0, 360], \phi \in [-90, 90]\}$. The objective function, f, for which the best beam ensemble is attained at the function's minimum has been considered by us as the optimal value of the FMO problem. Here, the optimal value of the DAO problem described in the previous section will guide the noncoplanar BAO search. In a noncoplanar setting, some beam directions cannot be considered as collision between gantry and couch or patient may occur. To accomplish this situation, the objective function f is formulated as

$$f((\theta_1, \phi_1), \dots, (\theta_n, \phi_n)) = \begin{cases} \text{optimal DAO value} & \text{if no collisions occur} \\ +\infty & \text{otherwise.} \end{cases}$$
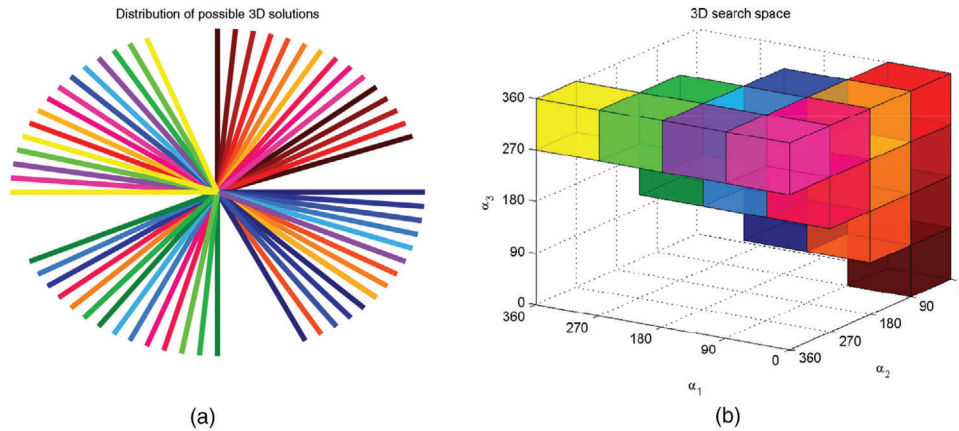
Fig. 2. All possible sorted combinations of three-beam ensembles divided by quadrant (a) and the corresponding cubes in the reduced 3D BAO search space (b).

In terms of BAO (or DAO) optimization, the order of each beam in the beam ensemble is irrelevant as all the beam ensembles with the same beam directions, even disposed in a different order, correspond to the exact same solution. Thus, the BAO search space can be largely reduced by keeping the beam directions sorted, reducing substantially the computational effort of the BAO search. To implement this strategy, the overall search space is split into hypercubes of one quadrant length. For illustration purposes, Fig. 2a represents all the possible combinations of three-beam ensembles by quadrant. In Fig. 2b, the corresponding cubes (reduced search space) are depicted. For example, the brown cube $[0, 90] \times [0, 90] \times [0, 90]$ in the 3D search space—Fig. 2b—corresponds to the brown three-beam ensemble in Fig. 2a where all the beams are in the first quadrant. This partition of the reduced search space proved to be useful for a straightforward multistart sampling strategy that considers an initial beam ensemble for each of the hypercubes. Depending on the dimension of the optimization problem (the number of beams), each of the hypercubes is still a large search region, with possibly many local minima, which should be explored resorting to derivative-free optimization methods to avoid local entrapment (Rocha et al., 2013a, 2013b, 2013c). Furthermore, each of the hypercubes can be considered as a region of attraction to prevent overlapping of the local hypercube searches. Algorithms 1 and 2 depict the derivative-free algorithm to locally explore each hypercube and the multistart algorithm, respectively. For further details, see Rocha et al. (2016, 2019a).

3.3. Noncoplanar arc trajectory optimization

The optimization approach proposed for calculating noncoplanar arc trajectories is anchored in the beam directions obtained by the BAO algorithm, adding iteratively novel anchor directions considering optimal DAO values. When 20 anchor beams are obtained, which is the typical number of anchor beams considered in the literature to define the trajectory path (Papp et al., 2015; Wild et al., 2015), this iterative procedure ends. In this work, we consider the concept introduced by

---

Algorithm 1. Parallel derivative-free algorithm

Initialization:

- Set $k \leftarrow 0$;
- Set $\mathbf{x}^0$ as the current best beam ensemble of a given hypercube;
- Set α_0 as the current step-size parameter for the corresponding hypercube;
- Set α_{min} to the same value defined in Algorithm 2;

Iteration:

1. Compute in parallel $f(\mathbf{x})$, the optimal DAO value, for all beam ensembles $\mathbf{x}$: $\mathbf{x} \in \mathcal{N}(\mathbf{x}^k) = \{\mathbf{x}^k \pm \alpha_k v_j, v_j \in [I \ - I]\}$, where $I = [e_1 \dots e_n]$ is the identity matrix.
2. If $\min_{\mathcal{N}(\mathbf{x}^k)} f(\mathbf{x}) < f(\mathbf{x}^k)$ then
   $\mathbf{x}^{k+1} \leftarrow \operatorname{argmin}_{\mathcal{N}(\mathbf{x}^k)} f(\mathbf{x})$;
   $\alpha_{k+1} \leftarrow \alpha_k$;
   Else
   $\mathbf{x}^{k+1} \leftarrow \mathbf{x}^k$;
   $\alpha_{k+1} \leftarrow \frac{\alpha_k}{2}$;
3. If $\alpha_{k+1} \geq \alpha_{min}$ return to step 1 for a new iteration and set $k \leftarrow k + 1$.

Unkelbach et al. (2015). According to these authors, in practice, an ideal benchmark treatment plan considering 180 beams may only be insignificantly better than considering 20 beams. It is thus possible to take a 360° arc, divided into 20 arc sectors of 18° each. This means that a high-quality VMAT treatment plan has the potential to approximate a high-quality 20-beam IMRT plan. VMAT does deliver an open field at a single gantry angle, but the total fluence delivered over an 18° arc sector can be thought of as an intensity-modulated field.

The methodological choices adopted in the current work guarantee a fair comparison between different approaches that were optimized under the same conditions using matRad. This software can only be used in a research environment, meaning that the obtained results cannot be immediately transposed to the clinical setting. However, some of the choices that were done, namely resorting to DAO, bridge the gap between the research environment and the clinical setting, strengthening the conclusions reached . The automated noncoplanar arc trajectory optimization is now described considering one of the head-and-neck cancer cases to illustrate the optimization strategy proposed.

Figure 3 displays in red, both in 2D (Fig. 3a) and in 3D (Fig. 3b), the 7-beam ensemble, solution of the noncoplanar BAO problem for one of the head-and-neck cancer cases tested. Note that each beam direction is represented by an ordered pair where the first coordinate refers to the gantry angle and the second to the couch angle. For the iterative optimization strategy proposed, an equispaced beam grid separated by 10° for both gantry and couch is considered and the corresponding beams are displayed in black for 0° couch angles, which typically corresponds to coplanar plans, or blue for different couch angle values. Infeasible beams due to possible collisions of couch and gantry for a head-and-neck cancer case were excluded as represented in Fig. 3.

Similar to the BAO approach, the arc trajectory optimization approach is based on dosimetric considerations, and will be guided by the optimal values of the DAO problem. Apart from geometric features, one of the criteria commonly used for calculating noncoplanar arc trajectories

---

Algorithm 2. Parallel multistart algorithm

Initialization:

- Set $k \leftarrow 0$;
- Choose the initial beam ensembles $\mathbf{x}_i^0$, one for each of the N hypercubes of the reduced search space;
- Compute $f(\mathbf{x}_i^0)$, $i = 1, \ldots, N$, the optimal DAO value for the initial beam ensembles, in parallel;
- Set the best beam ensembles as $\mathbf{x}_i^* \leftarrow \mathbf{x}_i^0$, $i = 1, \ldots, N$ and the best optimal DAO values in each hypercube as $f_i^* \leftarrow f(\mathbf{x}_i^0)$, $i = 1, \ldots, N$;
- Set all the hypercubes as regions of attraction having active local searches, $\mathbf{Active}_i \leftarrow 1$, $i = 1, \ldots, N$;
- Choose initial step-size, $\alpha_i^0 > 0$, $i = 1, \ldots, N$;
- Set α_{min} to the same value defined in Algorithm 1;

Iteration:

1. Use Algorithm 1 to locally explore the hypercubes with active local search;
2. For hypercubes i with active local search do
     If $f(\mathbf{x}_i^{k+1}) < f(\mathbf{x}_i^*)$ then
         If $\mathbf{x}_i^{k+1}$ is in cube i then
             $\mathbf{x}_i^* \leftarrow \mathbf{x}_i^{k+1}$;
             $f_i^* \leftarrow f(\mathbf{x}_i^{k+1})$;
         Else (local search "jump" to a different hypercube)
             $\mathbf{Active}_i \leftarrow 0$;
             Determine hypercube $j \neq i$ where $\mathbf{x}_i^{k+1}$ is;
             If $f(\mathbf{x}_i^{k+1}) < f(\mathbf{x}_j^*)$ then
                 $\mathbf{x}_j^* \leftarrow \mathbf{x}_i^{k+1}$;
                 $f_j^* \leftarrow f(\mathbf{x}_i^{k+1})$;
                 $\mathbf{Active}_j \leftarrow 1$;
     Else
         $\alpha_i^{k+1} \leftarrow \frac{\alpha_i^k}{2}$;
         If $\alpha_i^{k+1} < \alpha_{min}$ then
             $\mathbf{Active}_i \leftarrow 0$;
3. If there exists active hypercubes return to step 1 and set $k \leftarrow k + 1$.

---

is delivery time. Aiming at enhancing one of the main VMAT features, short delivery times, the gantry/couch movements are constrained according to the following conditions:

- The initial gantry/couch position is the leftmost anchor beam in Fig. 3a, corresponding to the beam of the noncoplanar BAO solution with the lowest value of gantry angle.
- The anchor beam to visit next has the lowest gantry angle value among the ones that have not been visited yet.
- The final gantry/couch position is the rightmost anchor beam in Fig. 3a, corresponding to the beam of the noncoplanar BAO solution with the highest value of gantry angle.
- The gantry must always move toward the next anchor beam while the couch can move toward the next anchor beam or be halted.

By imposing these movement constraints, the arc trajectory is defined from the leftmost anchor beam to the rightmost anchor beam of Fig. 3a as fast as possible, that is, with the gantry always
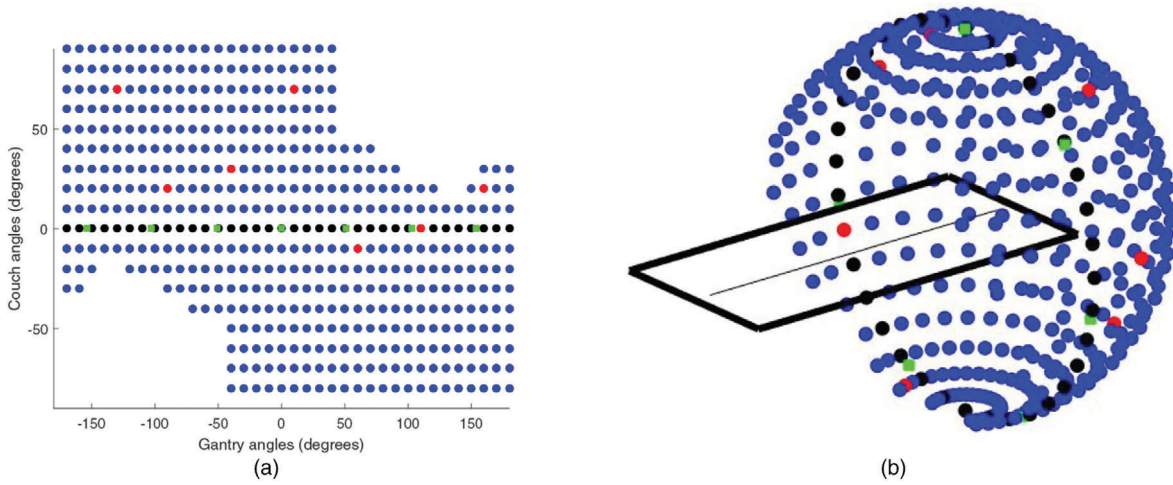
Fig. 3. Equispaced beam grid represented in 2D (a) and the corresponding 3D representation (b). Red beams correspond to the BAO solution, green beams to the 7-beam coplanar equispaced solution, black beams correspond to 0° couch angles (coplanar plans) while blue beams correspond to different couch values.
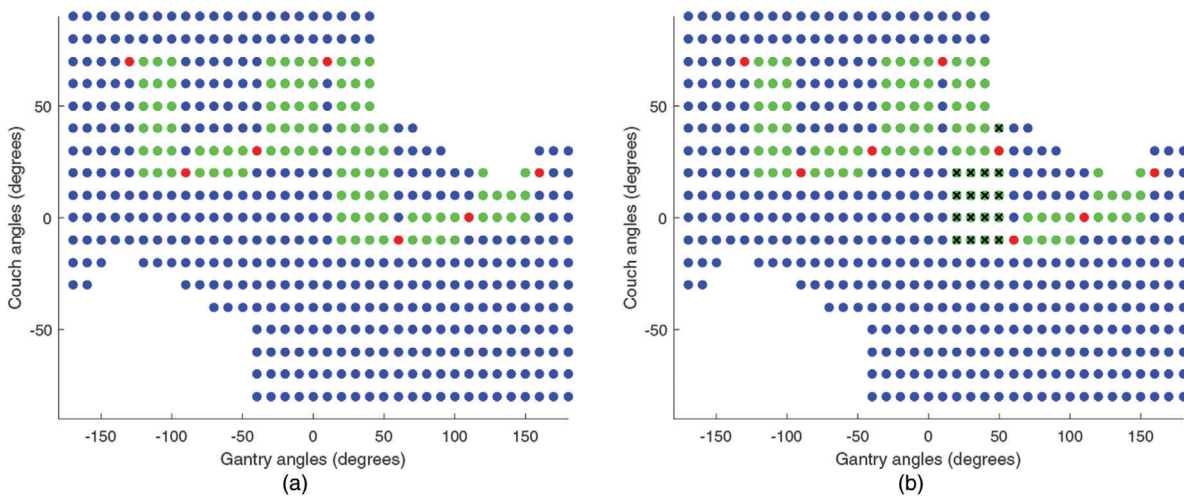

Fig. 4. The 7-beam noncoplanar BAO solution is displayed in red and the feasible points to consider when calculating a new anchor beam are displayed in green (a). Novel anchor beam belonging to the largest set of green candidate beams is added and green candidate beams that became infeasible are removed (b).

moving toward the next anchor beam and the couch also moving (when necessary) toward the next anchor beam. These movement constraints present yet another advantage. The number of feasible beams is considered when computing the next anchor beam is reduced. The candidate beams to consider when calculating a new anchor beam are shown in green in Fig. 4a. The most populated set is selected for searching the new anchor beam to add to the current arc trajectory. The rationale behind this idea is threefold: to reduce the computational time, to add anchor beams

where more degrees of freedom exist, and to reduce as much as possible the overall number of green points. After selecting the set of beams to test, each candidate beam is temporarily inserted in the trajectory and the optimal DAO value for the corresponding beam ensemble is calculated. The beam ensemble reporting the best performance is selected to become the updated arc trajectory. Then, the sets of eligible beams are updated and the largest one is selected for searching the new beam to add to the current arc trajectory. Figure 4b illustrates one iteration of this arc trajectory optimization approach. This iterative procedure ends when the number of anchor beams is 20. The process of obtaining the optimized arc trajectory has been completely automated in order to get the required solution without additional human intervention. The pseudocode of the arc trajectory optimization algorithm is presented in Algorithm 3.

4. Computational results

An eight-core Dell Precision T5600 with Intel Xeon processador was used and the computational tests were hosted by matRad workstation and Matlab 9.5. Objective functions displayed in Equation (1) were implemented in matRad by selecting the appropriate options. While dose calculation and fluence optimization is done using matRad, BAO (Algorithms 1 and 2) and arc trajectory optimization (Algorithm 3) were entirely developed and implemented by the authors, resorting to the matRad engine to perform the fluence calculations. In this work, a dose grid resolution of 2 mm $\times$ 2 mm $\times$ 3 mm was used. The beamlet width was set to 5 mm. Algorithms 1 and 2 considered $\alpha_0 = 2^5 = 32$ as an initial step size and define, as stopping criteria, a step size inferior to 1. By choosing a power of 2 for initial step size and 1 for minimum step size, all beam angle directions considered will be integer since the step size is divided by 2 in case of an unsuccessful local search.

The quality of the treatment plans obtained by the automated framework, called *ncVMAT*, was compared with coplanar VMAT plans, called *cVMAT*, with static noncoplanar IMRT plans considering the beam ensembles obtained by the BAO procedure, called *ncIMRT*, and with equispaced coplanar static IMRT plan, called *cIMRT*, still commonly used in clinical practice. Both coplanar and noncoplanar IMRT plans used seven beams. Figure 5 displays the highly noncoplanar trajectory obtained by our arc trajectory optimization framework.

The comparison of the different approaches was performed in terms of the optimal objective function value as well as resorting to different dosimetric measures typically used to assess the quality of treatment plans. The optimal FMO values obtained for each of the approaches tested are presented in Table 2. *ncVMAT* treatment plans clearly outperform the other treatment plans in terms of optimal FMO value, improving on average 32.4% of the value obtained by the benchmark treatment plan, *cIMRT*, while the improvements of *ncIMRT* and *cVMAT* were 19.0% and 27.1%, respectively. The average number of aperture shapes per beam is similar for all the approaches, ranging from 10 for *cIMRT* and *ncIMRT* to 10.54 and 10.77, for *cVMAT* and *ncVMAT*, respectively.

The objective function used can be interpreted as a technical tool that will guide the search process toward interesting regions of the search space, leading to high-quality treatment plans. However, the objective function value in itself does not have any clinical meaning, and it cannot be used alone to assess the quality of the treatment plan. Despite the excellent results obtained in terms of optimal objective function values, it is not possible to fully correlate its value with physical dose

---

Algorithm 3. Noncoplanar arc trajectory algorithm

Initialization:

- Set *anchorgantry* ← gantry angles correspondent to the BAO solution found
- Set *anchorcouch* ← couch angles correspondent to the BAO solution found
  - ○ Set s ← grid beam spacing
  - ○ Set $M(i, j) = 1, i = 1, \ldots, \frac{180}{s} + 1, \; j = 1, \ldots, \frac{360}{s}$
  - ○ Set $M(i, j) = 0$, for beams (i, j) where collision between gantry and patient may occur
- Set a ← number of beams of the BAO solution found
- Set T ← total number of beams of the final arc trajectory

Iteration:

While candidate beams exist **and** $a < T$ **do**

1. Identify the largest set, k, of candidate green beams between two consecutive anchor beams
   For $t = 1, \ldots, a - 1$
       $greenpoints(t) \leftarrow 0$
       $cMin \leftarrow \min\{anchorcouch(t), anchorcouch(t + 1)\}$
       $cMax \leftarrow \max\{anchorcouch(t), anchorcouch(t + 1)\}$
       $gMin \leftarrow \min\{anchorgantry(t), anchorgantry(t + 1)\}$
       $gMax \leftarrow \max\{anchorgantry(t), anchorgantry(t + 1)\}$
       For $c = cMin, \ldots, cMax$
         For $g = gMin + 1, \ldots, gMax - 1$
           $greenpoints(t) \leftarrow greenpoints(t) + M(c, g)$
         End
       End
   End
   $k \leftarrow arg \max(greenpoints)$
2. Select a new anchor beam from the set k, to add to the arc trajectory
   $selectedbeam \leftarrow \{\}$
   $fDAO_{min} \leftarrow \infty$
   For each beam i in set k
       $testbeams \leftarrow$ anchor beams $\cup$ beam i
       Compute the optimal DAO value, $fDAO$ of testbeams;
       If $fDAO < fDAO_{min}$
         $selectedbeam \leftarrow$ beam i
       End
   End
   Set $anchorgantry(a + 1) \leftarrow$ the gantry angle of selectedbeam i
   Set $anchorcouch(a + 1) \leftarrow$ the couch angle of selectedbeam i
   $a \leftarrow a + 1$

---

objectives or clinical response. Other metrics are typically used to assess the quality of treatment plans: D_{95} for the PTVs and maximum and mean doses for the serial and parallel OARs, respectively. D_{95} measures the dose delivered to at least 95% of the PTVs. D_{95} should be at least 95% of the prescribed dose. Comparison of PTV coverage metrics (D_{95}) obtained by *cIMRT*, *cVMAT*, *ncIMRT*, and *ncVMAT* treatment plans is displayed in Fig. 6, while comparison of organ sparing metrics is displayed in Fig. 8. The dose delivered for PTV_{70} near the maximum dose D2% is also
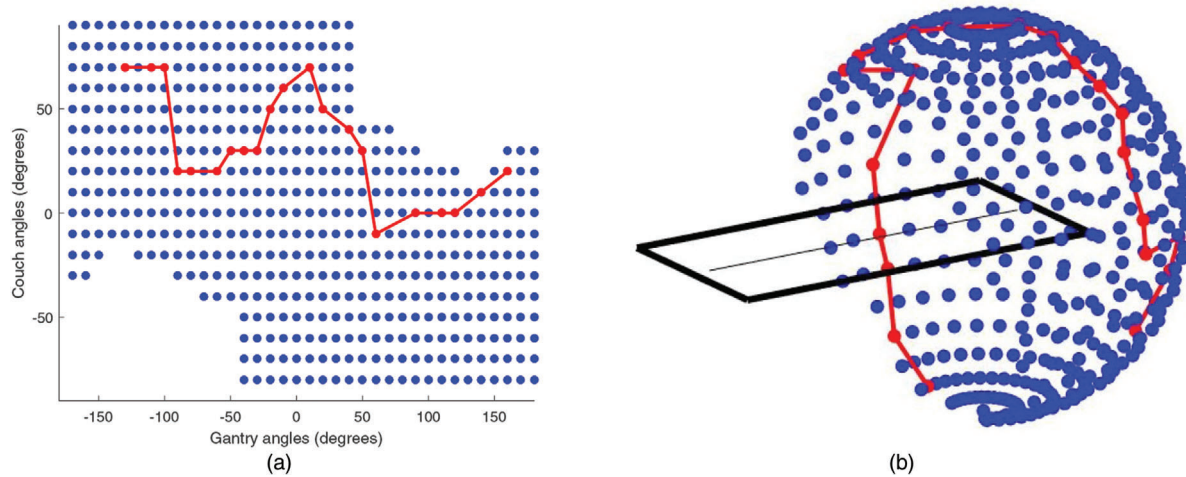
Fig. 5. Trajectory obtained by the noncoplanar arc trajectory optimization framework in 2D (a) and in 3D (b).

Table 2
Results in terms of optimal FMO value for the 12 cases

Case	cIMRT FMO value	cVMAT FMO value	% Decrease	ncIMRT FMO value	% Decrease	ncVMAT FMO value	% Decrease
1	140.0	132.3	5.5	138.1	1.4	129.7	7.4
2	45.7	30.8	32.6	38.6	15.5	29.7	35.0
3	235.6	219.5	6.8	220.3	6.5	213.4	9.4
4	180.9	159.5	11.8	171.5	5.2	157.4	13.0
5	68.0	41.2	39.4	47.8	29.7	40.5	40.4
6	111.2	100.3	9.8	105.2	5.4	101.1	9.1
7	63.0	45.6	27.6	60.8	3.5	41.5	34.1
8	41.3	25.5	38.3	25.6	38.0	22.0	46.7
9	8.1	7.0	13.6	7.2	11.1	5.9	27.2
10	37.3	24.4	34.6	25.6	31.4	20.8	44.2
11	32.2	20.0	37.9	21.2	34.2	15.8	50.9
12	40.9	13.4	67.2	21.9	46.5	11.5	71.9

provided in Fig. 7. It is possible to observe that in terms of coverage metrics both for tumor (PTV_{70}) and lymph nodes ($PTV_{59.4}$), *ncVMAT* clearly outperforms the remaining approaches. In terms of organ sparing, results obtained by the different plans fulfill most of the times the tolerance doses with no clear advantage of one approach for all the structures. For instance, for spinal cord *ncV-MAT* obtained the best sparing with an average of 1.5 Gy decrease with respect to the benchmark treatment plan, *cIMRT*, while for brainstem *cVMAT* obtained the best sparing with an average of 0.5 Gy decrease with respect to *cIMRT*. Note that plans with noncoplanar optimized directions are particularly suited for parotid sparing. For left and right parotids, *ncVMAT* obtained an average of 1.5 Gy and 1.0 Gy decrease with respect to *cIMRT* and *cVMAT*, respectively.
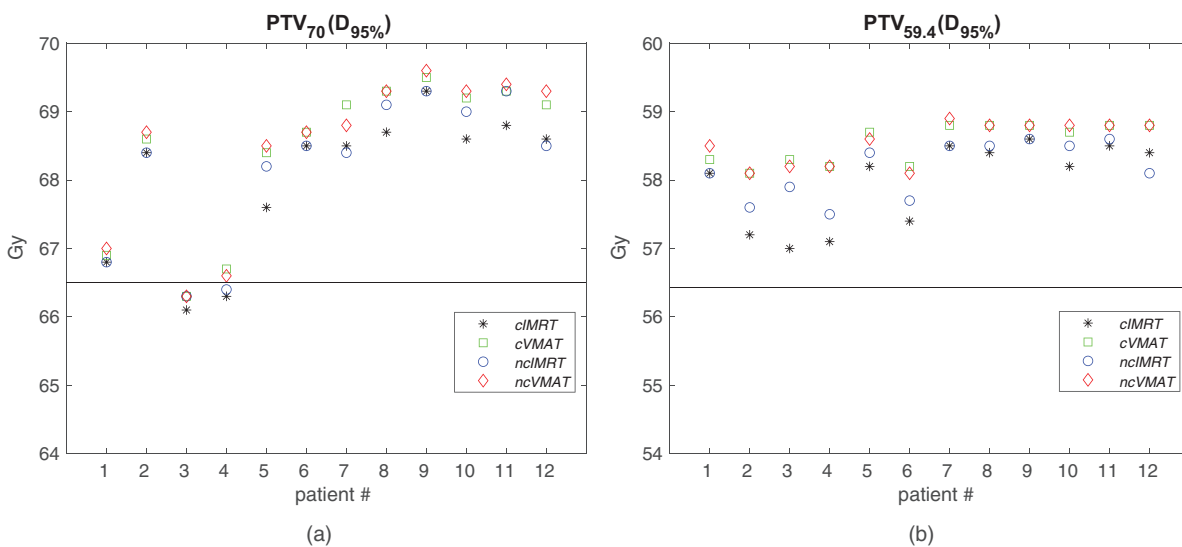
Fig. 6. Comparison of PTV coverage metrics (D_{95}) obtained by *cIMRT*, *cVMAT*, *ncIMRT*, and *ncVMAT* treatment plans. The horizontal lines displayed represent D_{95}.
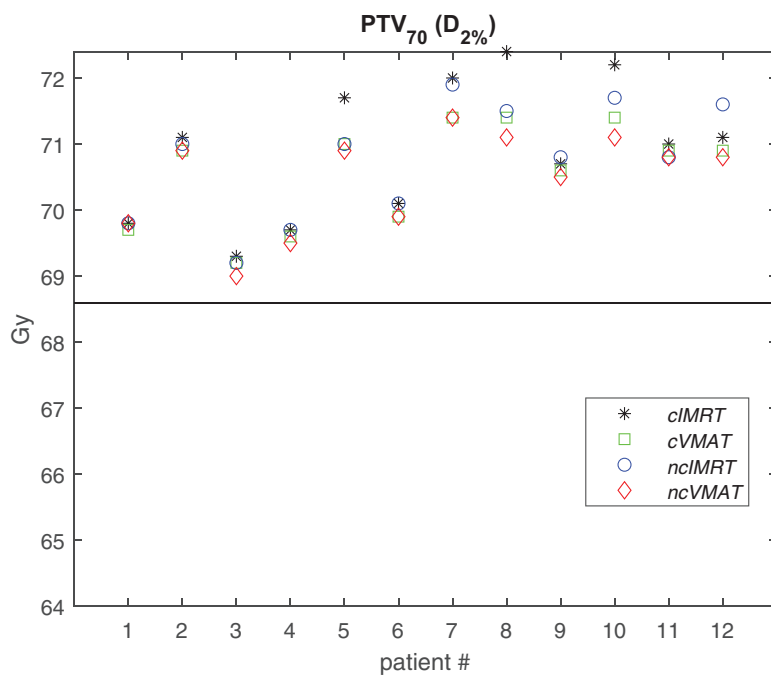

Fig. 7. Comparison of PTV coverage metric (D2) obtained by *cIMRT*, *cVMAT*, *ncIMRT*, and *ncVMAT* treatment plans. The horizontal line displayed represents 98% of the prescribed dose.
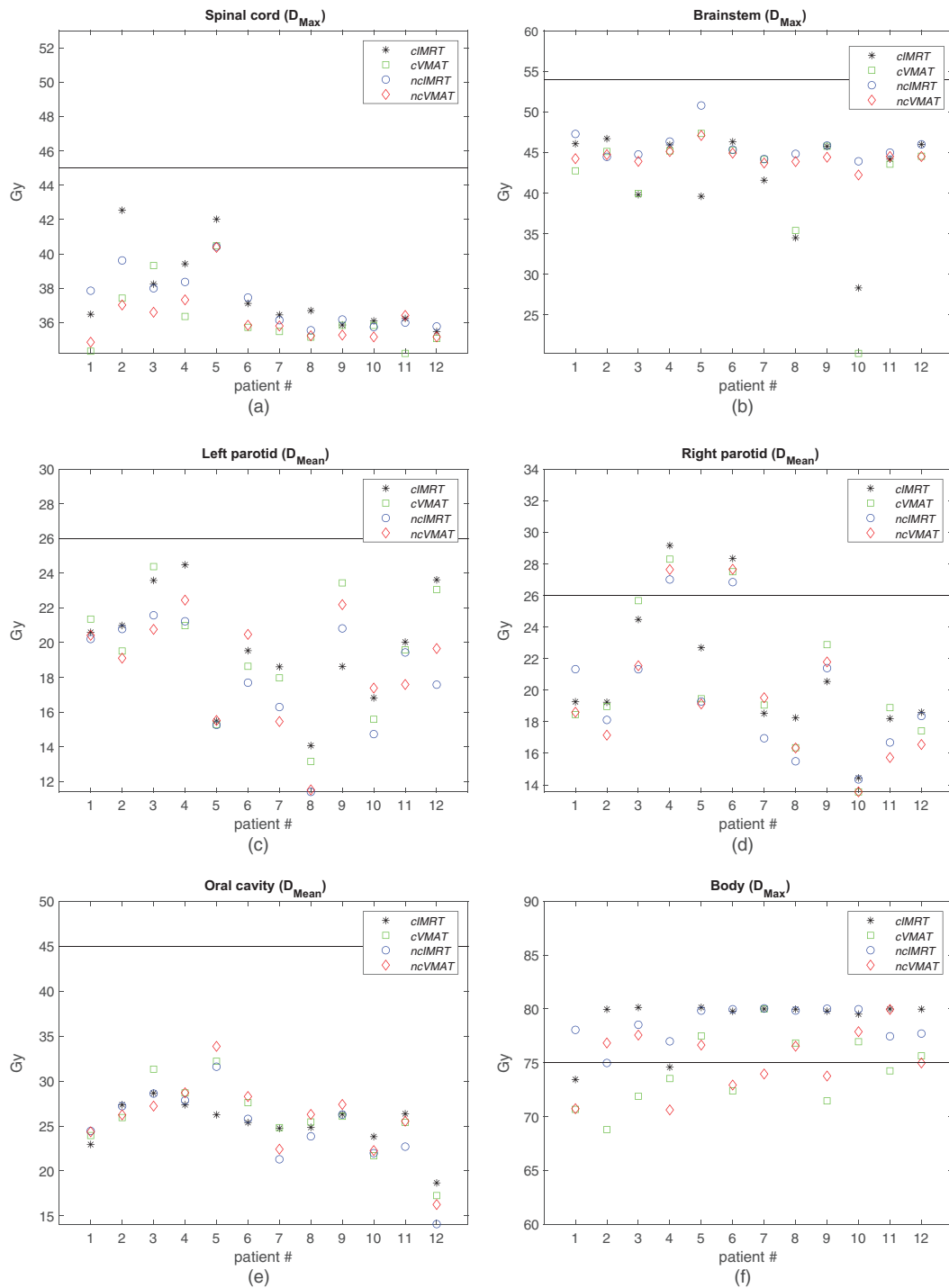
Fig. 8. Comparison of organ sparing metrics obtained by *cIMRT*, *cVMAT*, *ncIMRT*, and *ncVMAT* treatment plans.
The horizontal lines displayed represent the tolerance (mean or maximum) dose for each structure.

5. Conclusions

In this paper, a novel automated framework was proposed to determine optimized noncoplanar arc trajectories to deliver RT to cancer patients. Two problems that are very challenging on their own, the noncoplanar beam angle selection and the noncoplanar arc trajectory optimization, were combined in the proposed optimization framework. Both optimization procedures were guided by the optimal values of an experimental DAO implementation provided by matRad, aiming at minimizing discrepancies between research results and fully deliverable VMAT plans. All the treatment plans calculated and presented in the previous section took less than 12 hours of computational time. This is compatible with the clinical practice, especially considering that is a totally automated process, which does not require any intervention from the human planner. It is possible to run these procedures over the night, for instance.

The quality of the treatment plans obtained by the automated framework, *ncVMAT*, was assessed using a pool of 12 difficult head-and-neck cancer cases already treated at IPOC. Comparison with coplanar VMAT plans, *cVMAT*, noncoplanar IMRT plans, *ncIMRT*, and benchmark equispaced coplanar IMRT plans, *cIMRT*, was clearly favorable in terms of optimal objective function values obtained. In terms of dosimetric measures typically inspected to assess the quality of a treatment plan, *ncVMAT* also outperforms clearly the remaining approaches. In terms of organ sparing, the results are not so clear with advantage of different approaches for different structures and for different patients. Nevertheless, for some patients *ncVMAT* obtained the best results not only in terms of target coverage but also in terms of organ sparing for most of the OARs. For instance, for patient two, *ncVMAT* obtained not only better target coverage results than the remaining approaches but also better sparing of spinal cord, brainstem, left parotid, and right parotid. The selection of appropriate irradiation directions proved to be important for this particular case. The rules that were defined in defining the arc trajectory assure that the gantry/couch movements are minimized, being the number of these movements one of the main determinants of total delivery time. The effectiveness of the chosen strategy in terms of clinical delivery time has to be validated in clinical practice, which is beyond the scope of this work.

In Europe, currently, less than 75% of the patients that should be treated with radiotherapy, actually are (Lievens et al., 2019). One of the reasons is the time required for treatment planning of complex tumor cases that is still nowadays a trial-and-error process that can take from long hours to days for a medical physicist to complete. Automated procedures will not only simplify the current treatment workflow, making better use of the existing human resources, but they will also allow unbiased comparisons between different treatment techniques. The herein proposed approach is an early-stage contribution for automated noncoplanar arc trajectory optimization. It is possible to conclude that this automatic procedure does not jeopardize treatment quality for any patient, and can result in significant improvements for some particularly challenging cases. These results were obtained within a research environment context, and cannot be immediately transposed to the clinical context. However, considering the methodological choices made that bridge the gap between the research and the clinical setting, it is possible to conclude that automated procedures can be seen as an added-value for the clinical routine, and that it is worth it to invest in the clinical validation of these approaches.

Acknowledgments

References

Aleman, D., Kumar, A., Ahuja, R., Romeijn, H., Dempsey, J., 2008. Neighborhood search approaches to beam orientation optimization in intensity modulated radiation therapy treatment planning. *Journal of Global Optimization* 42, 587–607.

Atun, R., Jaffray, D., Barton, M., Bray, F., Baumann, M., Vikram, B., Hanna, T., Knaul, F., Lievens, Y., Lui, T., 2015. Expanding global access to radiotherapy. *The Lancet Oncology* 16, 1153–1186.

Bangert, M., Ziegenhein, P., Oelfke, U., 2012. Characterizing the combinatorial beam angle selection problem. *Physics in Medicine and Biology* 57, 6707–6723.

Bangert, M., Ziegenhein, P., Oelfke, U., 2013. Comparison of beam angle selection strategies for intracranial IMRT. *Medical Physics* 40, 011716.

Bertsimas, D., Cacchiani, V., Craft, D., Nohadani, O., 2013. A hybrid approach to beam angle optimization in intensity-modulated radiation therapy. *Computers & Operations Research* 40, 2187–2197.

Cabrera, G., Ehrgott, M., Andrew J.Mason, A.J., Raith, A., 2018. A matheuristic approach to solve the multiobjective beam angle optimization problem in intensity-modulated radiation therapy. *International Transactions in Operational Research* 25, 243–268.

Cassioli, A., Unkelbach, J., 2013. Aperture shape optimization for IMRT treatment planning. *Physics in Medicine and Biology* 58, 301–318.

Craft, D., 2007. Local beam angle optimization with linear programming and gradient search. *Physics in Medicine and Biology* 52, 127–135.

Dias, J., Rocha, H., Ferreira, B., Lopes, M., 2014. A genetic algorithm with neural network fitness function evaluation for IMRT beam angle optimization. *Central European Journal of Operations Research* 22, 431–455.

Dias, J., Rocha, H., Ferreira, B., Lopes, M., 2015. Simulated annealing applied to IMRT beam angle optimization: a computational study. *Physica Medica* 31, 747–756.

Freitas, J., Florentino, H., Benedito, A., Cantane, D., 2020. Optimization model applied to radiotherapy planning problem with dose intensity and beam choice. *Applied Mathematics and Computation* 387. https://doi.org/10.1016/j.amc.2019.124786.

Langhans, M., Unkelbach, J., Bortfeld, T., Craft, D., 2018. Optimizing highly noncoplanar vmat trajectories: the novo method. *Physics in Medicine and Biology* 63, 025023.

Lievens, Y., Ricardi, U., Poortmans, P., Verellen, D., Gasparotto, C., Verfaillie, C., Cortese, A., 2019. Radiation oncology. optimal health for all, together. ESTRO vision, 2030. *Radiotherapy and Oncology* 136, 86–97.

Lim, G., Cao, W., 2012. A two-phase method for selecting IMRT treatment beam angles: branch-and-prune and local neighborhood search. *European Journal of Operational Research* 217, 609–618.

MacDonald, R.L., Thomas, C.G., 2015. Dynamic trajectory-based couch motion for improvement of radiation therapy trajectories in cranial SRT. *Medical Physics* 42, 2317–2325.

Otto, K., 2008. Volumetric modulated arc therapy: IMRT in a single gantry arc. *Medical Physics* 35, 310–317.

Papp, D., Bortfeld, T., Unkelbach, J., 2015. A modular approach to intensity-modulated arc therapy optimization with noncoplanar trajectories. *Physics in Medicine and Biology* 60, 5179–5198.

Pugachev, A., Li, G., Boyer, A., Hancock, S., Le, Q., Donaldson, S., Xing, L., 2001. Role of beam orientation optimization in intensity-modulated radiation therapy. *International Journal of Radiation Oncology, Biology, Physics* 50, 551–560.

Rocha, H., Dias, J., Ferreira, B., Lopes, M., 2013a. Beam angle optimization for intensity-modulated radiation therapy using a guided pattern search method. *Physics in Medicine and Biology* 58, 2939–53.

Rocha, H., Dias, J., Ferreira, B., Lopes, M., 2013b. Pattern search methods framework for beam angle optimization in radiotherapy design. *Applied Mathematics and Computation* 219, 10853–65.

Rocha, H., Dias, J., Ferreira, B., Lopes, M., 2013c. Selection of intensity modulated radiation therapy treatment beam directions using radial basis functions within a pattern search methods framework. *Journal of Global Optimization* 57, 1065–1089.

Rocha, H., Dias, J., Ventura, T., Ferreira, B., Lopes, M., 2016. A derivative-free multistart framework for an automated noncoplanar beam angle optimization in IMRT. *Medical Physics* 43, 5514–5526.

Rocha, H., Dias, J., Ventura, T., Ferreira, B., Lopes, M., 2019a. Beam angle optimization in IMRT: are we really optimizing what matters? *International Transactions in Operational Research* 26, 908–928.

Rocha, H., Dias, J., Ventura, T., Ferreira, B., Lopes, M., 2019b. An optimization approach for noncoplanar intensity-modulated arc therapy trajectories. 19th International Conference on Computational Science and Its Applications, LNCS. Springer, Berlin, pp. 199–214.

Smyth, G., Bamber, J., Evans, P., Bedford, J., 2013. Trajectory optimisation for dynamic couch rotation during volumetric modulated arc radiotherapy. *Physics in Medicine and Biology* 58, 8163–8177.

Smyth, G., Evans, P., Bamber, J., Mandeville, H., Welsh, L., Saran, F., Bedford, J., 2016. Non-coplanar trajectories to improve organ at risk sparing in volumetric modulated arc therapy for primary brain tumors. *Radiotherapy and Oncology* 121, 124–131.

Unkelbach, J., Bortfeld, T., Craft, D., Alber, M., Bangert, M., Bokrantz, R., Chen, D., Li, R., Xing, L., Men, C., Nill, S., Papp, D., Romeijn, E., Salari, E., 2015. Optimization approaches to volumetric modulated arc therapy planning. *Medical Physics* 42, 1367–1377.

Wachter, A., Biegler, L., 2006. On the implementation of an interior-point filter line-search algorithm for large-scale nonlinear programming. *Mathematical Programming* 106, 25–57.

WHO, 2020. Cancer tomorrow. Available at http://gco.iarc.fr/tomorrow/home (accessed 2 October 2020).

Wieser, H.P., Cisternas, E., Wahl, N., Ulrich, S., Stadler, A., Mescher, H., Muller, L., T., K., Gabrys, H., Burigo, L., Mairani, A., Ecker, S., Ackermann, B., Ellerbrock, M., Parodi, K., Jakel, O., Bangert, M., 2017. Development of the open-source dose calculation and optimization toolkit matRad. *Medical Physics* 44, 2556–2568.

Wild, E., Bangert, M., Nill, S., Oelfke, U., 2015. Noncoplanar VMAT for nasopharyngeal tumors: plan quality versus treatment time. *Medical Physics* 42, 2157–2168.

Xia, P., Verhey, L., 1998. Multileaf collimator leaf sequencing algorithm for intensity modulated beams with multiple static segments. *Medical Physics* 25, 1424–1434.

Yang, Y., Xing, L., 2004. Inverse treatment planning with adaptively evolving voxel-dependent penalty scheme. *Medical Physics* 31, 2839–2844.

Yang, Y., Zhang, P., Happersett, L., Xiong, J., Yang, J., Chan, M., Beal, K., Mageras, G., Hunt, M., 2011. Choreographing couch and collimator in volumetric modulated arc therapy. *International Journal of Radiation Oncology, Biology, Physics* 80, 1238–1247.